



LUNDS UNIVERSITET  
Lunds Tekniska Högskola

# Dynamics of Mitochondria and Actin Cytoskeleton Interactions in Budding Yeast

*Master Thesis*

Martina Pola

August 2013

*Supervisors*

Prof. Liza Pon and Dr. Istvan Boldogh  
Department of Pathology and Cell Biology,  
Columbia University

*Examiner*

Prof. Leif Bülow  
Department of Pure and Applied  
Biochemistry, Lund University

## Rationale

Proper distribution of mitochondria is essential for cell survival. In the budding yeast, mitochondrial distribution is entirely dependent on the actin cytoskeleton. A great deal of information is known about how actin structures affect mitochondrial distribution, but less is known about how mitochondria influence the state of actin cytoskeleton. Here, I provide some evidence that the state of mitochondria also has an affect on actin structures.

## Abstract

In the budding yeast, *S. cerevisiae*, mitochondrial distribution involves movements of the organelle from the mother cell to the bud (anterograde movement) and from the bud to the mother (retrograde movement). Both types of movements require actin cables, dynamic bundles of F-actin filaments, which undergo continuous retrograde flow from the bud into the mother and provide tracks for mitochondrial movement. Some of the molecular mechanisms of these movements have been revealed: (1) retrograde movement of mitochondria is characterized by passive travel on actin cables using the actin-binding action of the mitochore/ERMES complex; (2) anterograde movement of mitochondria against the retrograde flow of actin cables requires an actin polymerization-dependent mechanism that include the actions of Arp2/3 complex, Jsn1p and Aim7p.

Much less is known about how the dynamic interactions at the interface between mitochondria and actin cytoskeleton affect the stability and maintenance of actin cables. Here we show that deletion of *ARC15*, a non-essential component of Arp2/3 complex, results in decreased actin cable abundance. Deletion of *AIM7* causes a decrease in retrograde actin cable flow. We also show that mitochondrial mass can influence the maintenance of actin cables. Cells grown under conditions where mitochondrial mass is modulated show different levels of actin cable thickness: there is an increase in actin cable thickness in cells with higher mitochondrial mass. This observation suggests that not only does the actin cytoskeleton affect mitochondrial distribution, but reciprocally, mitochondrial distribution can also affect the actin cytoskeleton. In case of cells with more mitochondria, changes in actin cable thickness seem to be essential to meet the demands of increased mitochondrial mass.

## Table of Contents

<b>1</b>	<b>Introduction.....</b>	<b>4</b>
1.1	<i>Mitochondrial Inheritance .....</i>	5
1.2	<i>The Actin Cytoskeleton in Yeast.....</i>	5
1.3	<i>Mechanisms for Retrograde and Anterograde Mitochondrial Movements.....</i>	7
1.4	<i>Actin Dynamics at the Mitochondria-actin Cable Interface .....</i>	9
1.5	<i>Experimental Plan.....</i>	10
<b>2</b>	<b>Materials and Methods .....</b>	<b>12</b>
2.1	<i>Yeast Growth Conditions .....</i>	12
2.2	<i>Visualization of F-actin Cytoskeleton with Rhodamine-Phalloidin.....</i>	12
2.3	<i>Western Blot for Protein Analysis .....</i>	13
2.4	<i>Yeast Strain Construction for Aim7p Knock Out.....</i>	14
2.5	<i>Visualization and Analysis of Retrograde Actin Cable Flow with Abp140-GFP .....</i>	14
2.6	<i>Microscopy.....</i>	15
2.7	<i>Statistical Methods.....</i>	15
<b>3</b>	<b>Results and Discussion .....</b>	<b>16</b>
3.1	<i>Deletion of ARC15 Results in Decreased Actin Cable Abundance and Loss of Actin Patches.....</i>	16
3.2	<i>Deletion of AIM7 Results in Decreased Retrograde Actin Cable Flow.....</i>	16
3.3	<i>Growth in Non-fermentable Carbon Sources Results in Upregulation of Mitochondrial Proteins and Increases in Actin Cable Thickness .....</i>	19
<b>4</b>	<b>Conclusions and Further Directions .....</b>	<b>23</b>
<b>5</b>	<b>Acknowledgements.....</b>	<b>25</b>
<b>6</b>	<b>References.....</b>	<b>26</b>

# 1 Introduction

The yeast *Saccharomyces cerevisiae* has been used since ancient times for winemaking, baking and brewing. It reproduces by an asymmetric division process known as budding. The mechanism of nucleus inheritance has earlier extensively been studied and it is now clear that similar processes also occur for other organelles in the cell, such as the mitochondria. Since mitochondria are essential organelles for the cell it is of great importance to understand their inheritance process during cell division in budding yeast [1].

Mitochondria are found in almost all eukaryotic cells and are essential organelles for proper eukaryotic cell function. They are the site of many complex biochemical processes and are the primary source of energy for the cell. They are very dynamic and undergo constant fission and fusion. Mitochondria are only produced from preexisting mitochondria and when cells divide, mitochondria in the mother cell are inherited to the daughter cell. This is essential for daughter cell survival and cell proliferation [2].

The yeast *S. cerevisiae* is one of the most intensively studied eukaryotic model organisms in cell biology. Its simple life cycle, culture conditions, rapid growth and easily manipulatable genome make it a very suitable model organism. In fact, the budding yeast was the first eukaryote to have its genome sequenced. Mitochondrial inheritance and function during cell division have been studied also most extensively in the budding yeast. Since mitochondrial function and protein composition are conserved, studies of yeast mitochondria have been essential for a better understanding of mitochondrial functions in higher organisms [3, 4].

## 1.1 Mitochondrial Inheritance

*S. cerevisiae* grows and divides asymmetrically by budding and therefore the inheritance of mitochondria and other organelles from mother to daughter cells rely on an active segregation process. To enable this mitochondrial transfer a fraction of the mitochondria mobilizes and immobilizes at different stages of the cell cycle (Fig. 1) [5]. During Gap 1 ( $G_1$ ) phase mitochondria align along the mother-bud axis. In Synthesis (S) and Gap 2 ( $G_2$ ) phases - as the bud emerges and grows - some mitochondria are immobilized at the mother tip and some are transported and anchored at the bud tip. Mitochondria remains immobilized at the tips until the end of Mitosis (M) phase. Poleward mitochondrial movement together with immobilization at either mother or bud tip result in the equal segmentation of organelles between mother and daughter cells.

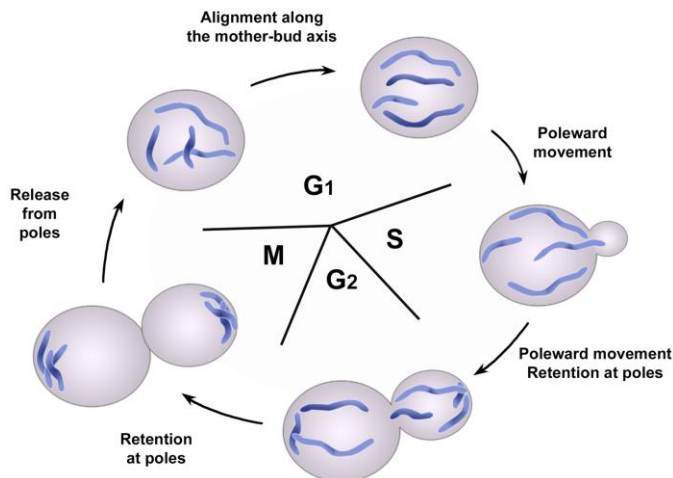


**Fig.1** Mitochondria undergo poleward movement and retention at the poles during yeast cell division. At  $G_1$  the mitochondria align along the mother-bud axis. During S phase the bud emerges and the mitochondria undergo linear poleward movement. Some mitochondria move towards the bud and some towards the distal tip of the mother cell. This continues during  $G_2$  and M phase. Mitochondria are immobilized at the bud or mother tip until the end of the cell division cycle when they are released. (Peraza-Reyes, L., Crider, D.G. and Pon, L.A., 2010)

## 1.2 The Actin Cytoskeleton in Yeast

The yeast cytoskeleton consists of microtubules and microfilaments, which serve as tracks for organelle movements. Microtubules are hollow, cylindrical polymers of

tubulin monomers extending throughout the cytoplasm. They are responsible for the inheritance of nucleus from the mother to the daughter cell [6]. Microfilaments consist of actin monomers that can be polymerized into F-actin filaments. In yeast many cellular organelles including endosomes, vacuoles, peroxisomes, and mitochondria require the actin cytoskeleton for normal distribution and inheritance [6].

In yeast there are two F-actin-containing structures that are essential throughout the cell division cycle, actin patches and actin cables (Fig. 2). Actin patches are endocytic vesicles decorated with short F-actin filaments and are localized in the growing bud. Actin cables are bundles of long F-actin filaments that extend from their assembly sites toward the distal tip of the mother [7]. Long F-actin filaments are nucleated and elongated at the bud tip and bud neck by two formin proteins, Bni1p and Bnr1p. The F-actin filaments thereafter are bundled into actin cables by actin-bundling proteins, fimbrin and Abp140p. The continuous F-actin filament assembly at the bud tip and neck results in a retrograde flow of actin cables towards the mother cell from the bud [8].

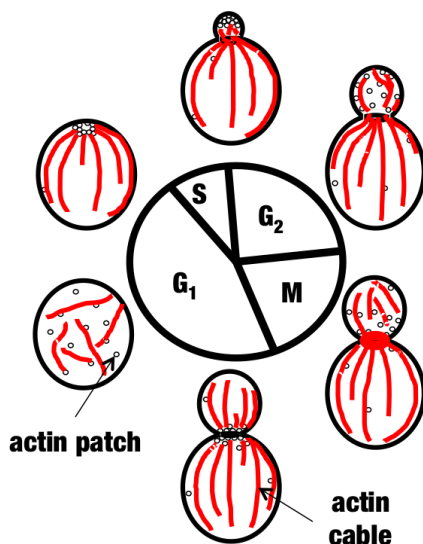


**Fig. 2** The actin cytoskeleton during the cell cycle. Actin cables are indicated in red and are bundles of actin filaments. They are randomly distributed in non-dividing yeast cells but are oriented along the mother-bud axis from late G<sub>1</sub> to M phase. Actin patches are indicated as small circles and they are endosomes decorated with actin filaments. (Yang, H.C. and Pon, L.A., 2002)

### **1.3 Mechanisms for Retrograde and Anterograde Mitochondrial Movements**

Early studies have shown that mitochondria colocalize with actin cables, and the presence of actin cables is essential for mitochondrial movement and distribution [9, 10]. There are two mechanisms for actin-based organelle motility: (1) motor dependent and (2) actin-polymerization (Arp2/3 complex) dependent. In motor-dependent movements the actin-binding motor molecule, myosin, binds to an organelle and to the lateral surface of actin filaments. As myosin moves along actin filaments it carries along the organelle. Some of the organelles that require myosin for transportation along actin cables include endoplasmic reticulum (ER), peroxisomes and vacuoles [11]. Interestingly, mitochondrial movement in yeast does not involve myosin, but requires other factors (see below) [12, 13].

During cell division mitochondrial movement towards the mother is referred to as retrograde movement while movement towards the bud as anterograde movement. Mitochondrial movements in both directions require the reversible binding of the organelle to actin cables. This binding is achieved by the mitochondrial outer membrane protein complex, the mitochore/ERMES (Fig. 3) complex [14, 15]. There are, however, important differences regarding the mechanisms of retrograde and anterograde movements. The retrograde mitochondrial movement is dependent on retrograde actin cable flow. Mitochondria bind to actin cables and use the forces of retrograde actin cable flow to drive their movement towards the distal tip of the mother cell, just as something is carried on a conveyor belt while being transported (see Fig. 3, upper panel).

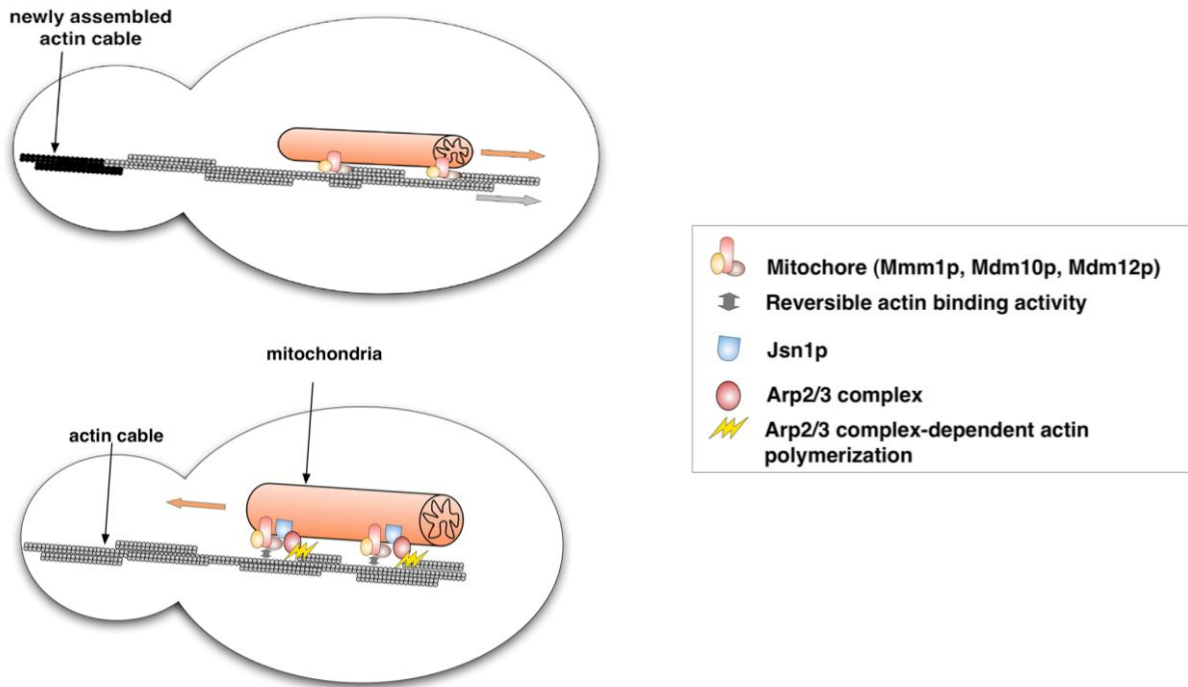


**Fig. 3** Upper panel shows retrograde mitochondrial movement. It is dependent on the retrograde actin cable flow, which is driven by actin polymerization. Lower panel shows anterograde mitochondrial movement. Jsn1p recruits the Arp2/3 complex, which generates a force to move the mitochondria towards the bud. (Boldogh, I.R., *et al.*, 2003)

For anterograde movement along actin cables, mitochondria have to overcome retrograde flow of actin cables. This force is generated by the Arp2/3 complex (see Fig. 3 lower panel). The Arp2/3 complex consists of two actin-related proteins, Arp2p and Arp3p, as well as five other associated subunits: Arc40p, Arc35p, Arc18p, Arc19p and Arc15p [16]. The Arp2/3 complex is highly conserved from *S. cerevisiae* to humans. In yeast and mammalian cells this complex localizes to endosomes where they contribute to cortical endosome movements [17]. Arp2/3 complex is also essential to the movements of several pathogenic bacteria including *Listeria*, *Shigella* and *Rickettsia* species inside the infected host cells [18]. These movements require the Arp2/3 complex at the surface of the organelle or pathogens. There the complex induces the polymerization of short actin filaments. The complex can also bind to preexisting actin filaments and nucleate branches at an angle of 70°. The actin filaments polymerized by Arp2/3 complex are branched and cross-linked into a comet-tail like network. The continuous assembly of the actin network at the membrane surface and the disassembly at the distal end of the comet-tail creates a pushing force for polarized intracellular movements of organelles and pathogens. In



yeast the Arp2/3 complex localizes to actin patches in the bud and neck and to mitochondria. Recruitment of Arp2/3 complex to mitochondria is dependent on the peripheral mitochondrial membrane protein Jsn1p, which localizes to punctuate structures on the mitochondria [19]. Deletion of *JSN1* decreases the amount of Arp2/3 complex to mitochondria. Also, deletion of *JSN1* results in decrease of the anterograde, but not the retrograde mitochondrial movements, a phenotype that is similar to the deletion of Arp2/3 complex.

#### **1.4 Actin Dynamics at the Mitochondria-actin Cable Interface**

Dynamic removal of branched actin network at the surface of mitochondria also seems to be an important component for mitochondrial motility. Earlier, using a genetic screen, a yeast protein, Aim7p, also known as glia maturation factor (GMF), has been identified to have a role in mitochondrial inheritance (aim=altered inheritance rate of mitochondria) [20]. Aim7p was also shown by Gandhi *et al.*, 2010 to bind tightly to Arp2/3 complex *in vitro* and to debranch the actin networks produced by Arp2/3 complex. These two observations suggested that debranching activity might be important for mitochondrial motility and therefore inheritance during cell division. Indeed, the deletion of *AIM7* resulted in decreased mitochondrial motility and less thick actin cables [28]. In addition, deletion of *AIM7* also resulted in a decrease in actin cable numbers. These observations led to the model whereby the branched F-actin network generated by the Arp2/3 complex is debranched by Aim7p. The resulting short filaments then are incorporated into actin cables to create efficient pushing force of the mitochondria towards the bud (Fig. 4).

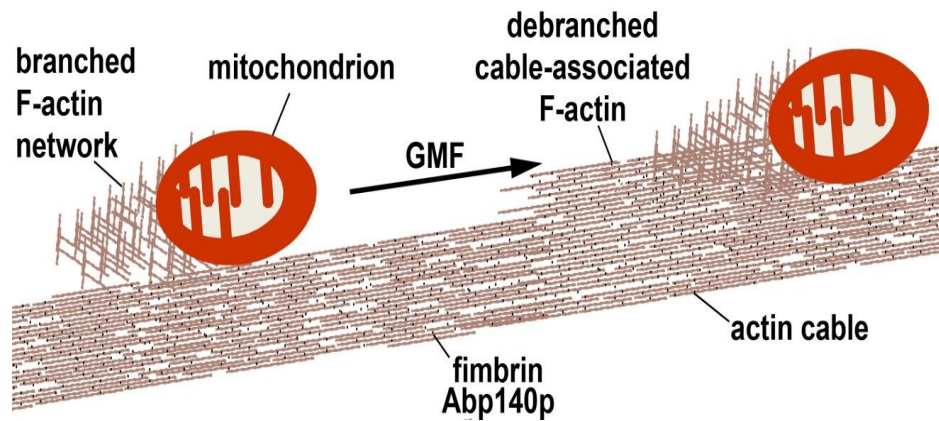


**Fig. 4** Debranching model for mitochondrial movement in anterograde direction. The branched F-actin network is generated by the Arp2/3 complex. Aim7p debranches this network, and resulting parallel filaments are incorporated into actin cables and thus create a pushing force of the mitochondria towards the bud. Figure in cooperation with the laboratory of Prof. Liza Pon.

Deletion of JSN1, a receptor for Arp2/3 complex at the surface of mitochondria, also resulted in decreased actin cable thickness and reduced actin cable number [28].

Altogether, these observations suggest that the dynamic interactions at the interface between mitochondria and actin cables are important factors for the stability and maintenance of the actin cables. Although there is no direct evidence of comet tails in yeast cells, actin clouds that are distinct from actin patches and actin cables can be seen around mitochondria in yeast [12]. These actin clouds might represent the branched F-actin network at the mitochondrial surface (Fig. 4).

### 1.5 Experimental Plan

To further explore how dynamic interactions at the interface between mitochondria and actin cables affect the stability and maintenance of the actin cables we investigated the role of Arc15p, a non-essential component of Arp2/3 complex, to actin cable stability. Earlier it was shown that a dysfunctional Arc15p reduces mitochondrial motility [12]. Here, I investigated whether the deletion of *ARC15* results in changes in actin cable structures.

If dynamic interactions between mitochondria and actin cables are important then we can expect that the amount of mitochondria in the cell affects the number, therefore the stability of actin cables. It has been known for a long time that yeast cells are facultative aerobic organisms, and the mitochondrial mass can be regulated by growing the cells under anaerobic or aerobic condition. During anaerobic growth, in the presence of a fermentable carbon source e.g. glucose, mitochondrial biogenesis is repressed. This condition is called glucose repression. In the presence of non-fermentable carbon sources such as lactic acid or glycerol, however, mitochondrial biogenesis is released from glucose repression and the organelle undergoes respiratory adaptation. This results in increased mitochondrial mass per cell volume [21]. Glucose repression is significant in regulation of energy homeostasis in yeast cells. During growth in high concentrations of glucose, glycolysis is the primary mechanism of energy production and mitochondrial enzymatic action is limited. Under de-repressing conditions such as growth in absence of glucose in non-fermentable carbon sources, mitochondrial biogenesis and enzymatic activity of key mitochondrial proteins are upregulated [22]. Here I investigated whether modulating the amount of mitochondria per cell results in changes in the number and/or stability of actin cables.

Surprisingly, *AIM7* deletion affects not only anterograde, but retrograde mitochondrial movements too [28]. This was an unexpected observation since retrograde mitochondrial movements require only the moving actions of actin cable flow. Here I investigated whether the flow of actin cables are changed in *aim7* deletion cells. A decrease in the velocity of actin cable flow would explain the decrease in retrograde mitochondrial velocity.

## 2 Materials and Methods

### 2.1 Yeast Growth Conditions

All *S. cerevisiae* strains used in this study are derivatives of the wild type BY4741 strain (*MATa his3Δ1 leu2Δ0 met15Δ0 ura3Δ0*) from Open Biosystems (Huntsville, AL). Yeast cells were cultivated and manipulated as described previously [4]. All imaging experiments were carried out with cultures grown to mid-log phase ( $OD_{600}$  0.1-0.3). Cells were grown at 30°C with shaking at 225 rpm unless otherwise noted. Standard rich medium (YPD) was used for growth of strains not requiring selection. For strains requiring selection, synthetic complete (SC) media with corresponding dropouts of essential nutrients were used. For all imaging studies with the exception of retrograde actin cable flow imaging, SC media was used with dropouts where needed. For retrograde actin cable flow imaging, lactate was used since fluorescence of Abp140-GFP was greater in this medium than in SC.

### 2.2 Visualization of F-actin Cytoskeleton with Rhodamine-Phalloidin

Cells at mid-log phase were concentrated at 10,000 rpm for 15 sec and fixed by incubation in 3.7% paraformaldehyde added directly to the growth medium at 30°C with shaking for 50 min. Fixed cells were washed three times with wash solution (0.025M KPi pH 7.5, 0.8M KCl), once with PBT (PBS containing 1% w/v BSA, 0.1% v/v Triton X-100, 0.1% w/v sodium azide), and stained for actin with 1.65μM rhodamine-phalloidin (Molecular Probes, Eugene, OR) for 35 min at room temperature in the dark. Cells were then washed three times with PBS, resuspended in mounting solution (0.1% w/v p-phenylenediamine and 90% v/v glycerol in PBS), mounted on microscope slides, and stored at -20°C until visualization.

F-actin imaging was performed with a 100x/1.3 EC Plan-Neofluar objective (Carl Zeiss Inc., Thornwood, NY). Rhodamine-phalloidin was imaged using a metal-halide lamp for excitation and a standard rhodamine filter (Zeiss filter set 43 HE; excitation 550/25, dichroic FT 570, emission 605/70). Z-series were collected through the entire cell at 0.3-μm intervals using 1x1 binning, 20 ms exposure, and analog gain at

216. Images were deconvolved using a constrained iterative restoration algorithm (Volocity, Perkin-Elmer, Waltham, MA) with the following parameters: 620nm excitation wavelength, 60 iterations, and 100% confidence interval. Cells with small and medium-sized buds were selected for quantification of actin polarization. These were defined as cells in which the ratio of bud length to mother length (measured from the neck to the bud or mother tip, respectively) was between 0.20 and 0.60. Thickness of actin cables was measured by drawing a line profile in ImageJ software. Line profiles are made through the ROI tool and drawn roughly perpendicular to the mother-bud axis near the middle of the mother cell, avoiding actin patches. Widths of the line profiles were measured at half-max peak height, and acquire measurements of actin cable thickness in  $\mu\text{ms}$ .

### **2.3 Western Blot for Protein Analysis**

Whole cell extract was prepared by vortexing mid-log phase yeast cells with 0.5-mm glass beads in a solution consisting of 10% glycerol, 10mM EGTA, 1% Triton X-100, 50mM Tris-HCl pH 7.5, 150mM NaCl, 2mM PMSF, and protease inhibitor cocktail [23]. Protein concentration of the lysate was determined by using the bicinchoninic acid assay following vendor's protocol (Pierce Chemical, Rockford, IL). Proteins were separated on SDS-PAGE, transferred onto PVDF membranes and immunoblotted with an antibody raised against porin,  $\alpha$ -Ketoglutarate and tubulin. Intensity of bands were measured and normalized against tubulin or trichloroethanol (TCE)-stained proteins as described [23]. Poly-acrylamide gels were made with 0.5% TCE (v/v) and visualized by UV exposure for 5 minutes. Visualization of proteins was accomplished with SuperSignal West Pico HRP substrate (Fisher, Woodside, California) on a BioRad ChemiDoc imager and confirmed by x-ray film development.

## 2.4 Yeast Strain Construction for Aim7p Knock Out

Knockout strains were created by replacing the gene of interest with *LEU2* cassettes using forward primer 5'TTAGTTTTGCAATTGCGTCCTCAAAGCATCGAGCAAA CAATCTGCAGGTCGACAACCCTTAAT3' and reverse primer 5'TATAGTCTATCTTAAACACTAAACTACCTCCTATAATCAT3'. For this experiment, genomic *AIM7* was replaced with *LEU2*. A PCR fragment containing regions homologous to sequences directly upstream of the start and stop codons of *AIM7* and coding regions for *LEU2* was amplified from plasmid POM13 (available from Addgene, Cambridge, MA) using listed primers. RHY050 (BY4741 with Abp140-GFP) cells were transformed with the PCR product using the lithium acetate method and transformants were selected on SC-Leu. The *aim7Δ* yeast strains were characterized for deletion by PCR using forward primer 5'CGCGGACAAAAGAAGAACATGT CAACGCC3' and reverse primer 5'CATACGGCACTGTGCATACGACCC3'.

## 2.5 Visualization and Analysis of Retrograde Actin Cable Flow with Abp140-GFP

For time-lapse fluorescence imaging of Abp140p-GFP, cells were grown in lactate medium [8] until mid-log phase at 30°C. 1.5μl of cell suspension was applied to a microscope slide and covered with a coverslip and imaged immediately for a maximum of 5 min after mounting. Microscopy was performed using a microscope (E600; Nikon) equipped with a Plan Apo ×100/1.4 NA objective and a cooled charge-coupled device camera (Orca-ER; Hamamatsu). Illumination with a 100 W mercury arc lamp was controlled with a shutter (Uniblitz D122; Vincent Associates). Images were collected and analyzed using Volocity software (Perkin-Elmer, Waltham, MA). The exposure time and time interval between successive image acquisitions were 300ms and 900ms, respectively. The total imaging time for the time-lapse imaging was 20 s. For determination of the velocity of elongating actin cables, the change in position of fluorescent fiduciary marks on elongating cables was measured as a function of time. Images were collected at a focal plane 0.5-1μm higher than the center of the mother cell.

## **2.6 Microscopy**

All fluorescence microscopy, with the exception of measurements of retrograde actin cable flow, was performed on a Zeiss AxioObserver.Z1 microscope (Carl Zeiss Inc., Thornwood, NY) equipped with a metal halide lamp and Colibri LEDs for excitation (Carl Zeiss), and an Orca ER cooled CCD camera (Hamamatsu Photonics, Bridgewater, NJ), and driven by Axiovision software (Carl Zeiss). Details are given with each imaging method. Fluorescence microscopy of retrograde actin cable flow was performed on an E600 Nikon microscope equipped with a Plan Apo  $\times 100/1.4$  NA objective and a cooled charge-coupled device camera (Orca-ER; Hamamatsu). Illumination with a 100 W mercury arc lamp was controlled with a shutter (Uniblitz D122; Vincent Associates).

## **2.7 Statistical Methods**

All statistical testing was performed using non-parametric testing. P-values for all data sets were determined using the non-parametric Kruskal-Wallis test. All statistical testing, production of box plots, and determination of p-values were carried out using the Analyze-it add-on for Microsoft Excel.

### 3 Results and Discussion

#### 3.1 Deletion of *ARC15* Results in Decreased Actin Cable Abundance and Loss of Actin Patches

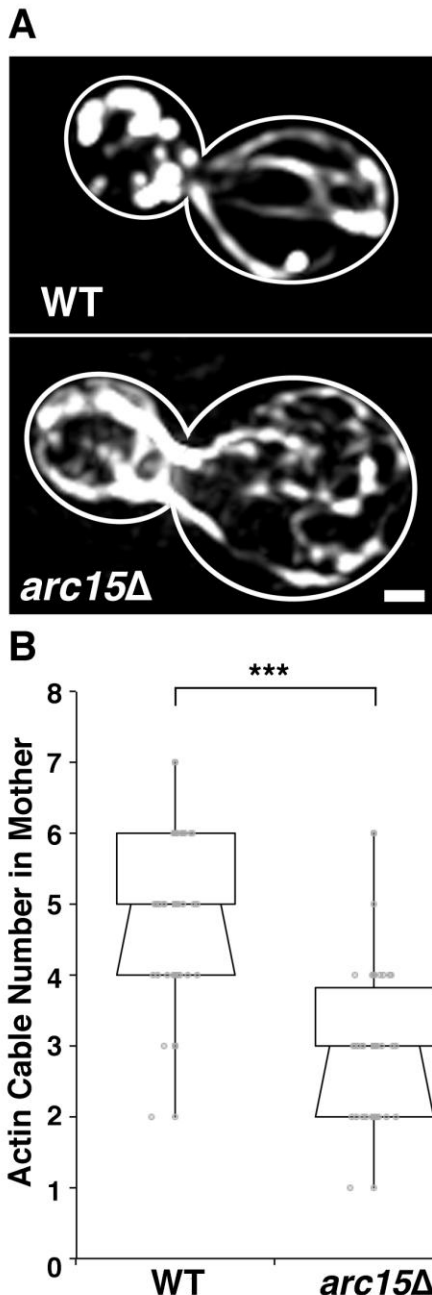
The Arp2/3 complex is involved in polymerization of actin cables in *S. cerevisiae* [24]. Because actin cables serve as a highway for mitochondrial movement within the cell, aberrations in the actin cytoskeleton often alter mitochondrial motility [8]. We analyzed the effect of deletion of *ARC15* on actin cable abundance and actin polarity. Rhodamine-phalloidin staining of actin cables and cortical actin patches revealed that actin cables are destabilized and appear as short, fragmented cables in the *arc15Δ* compared to wild-type cells. There are no detectable actin patches in both the mother and the bud in the *arc15Δ* compared to wild-type cells (Fig. 5A). Actin patches are endosomes decorated with actin filaments. The absence of actin patches suggests that either endocytosis, an actin-dependent mechanism, is perturbed or attachment of actin filaments to the endocytic vesicles does not occur in the *arc15Δ* cells. Indeed, there is a significant increase in generation time of *arc15Δ* cells, which may be due to defects in endocytosis (data not shown). Quantification of long, linear actin cables defined as those equal to or greater than the length of the mother cell, revealed actin cable abundance decreases from 4.82 in wild-type to 2.94 in *arc15Δ* cells (Fig. 5B).

#### 3.2 Deletion of *AIM7* Results in Decreased Retrograde Actin Cable Flow

Previous studies indicate that deletion of *AIM7*, an actin debranching protein, results in decrease of both anterograde and retrograde mitochondrial motility [28]. Aim7p binds to the Arp2/3 complex and stimulates debranching of actin filaments produced by the Arp2/3 complex, providing a forward force for anterograde mitochondrial movement [26]. We speculate that the loss of Aim7p decreases the available force for anterograde movement of mitochondria. To further explore the role of Aim7p on mitochondrial motility, we investigated the role of Aim7p on regulation of the actin cytoskeleton, which serve as tracks for mitochondria in yeast.



We find that deletion of *AIM7* results in decreased actin cable abundance and loss of actin polarity [28]. Indeed, disruption of the actin cytoskeleton results in defects in both anterograde and retrograde mitochondrial movement. To investigate the role of Aim7p on retrograde mitochondrial movement specifically, we looked at retrograde actin cable flow, the primary driving force for retrograde mitochondrial movement [9]. Deletion of *AIM7* results in a decrease in the velocity of retrograde actin cable flow from  $0.464\mu\text{m/s}$  in wild type to  $0.339\mu\text{m/s}$  in *aim7\Delta* (Fig. 6B). Thus, decreases in anterograde and retrograde mitochondrial motility correlate with



defects in the actin cytoskeleton, as assessed by actin cable abundance, actin polarity, and velocity of retrograde actin cable flow.

**Fig. 5** Deletion of *ARC15* results in decreased actin cable abundance and loss of actin patches. **(A)** Representative images of rhodamine-phalloidin stained actin of wild-type (KFY211) and *arc15\Delta* yeast cells. **(B)** Polarized, long actin cables were counted in mother cells bearing small to medium-sized buds (bud diameter 20-60% of the diameter of the mother cell). Polarized cables were defined as cables that are parallel to the mother-bud axis. Notched dot box plots where central bands in the box represent the median, boxes indicate the middle quartiles, and whiskers extend to the 5<sup>th</sup> and 95<sup>th</sup> percentile. n = 100, representative data of 3 trials.

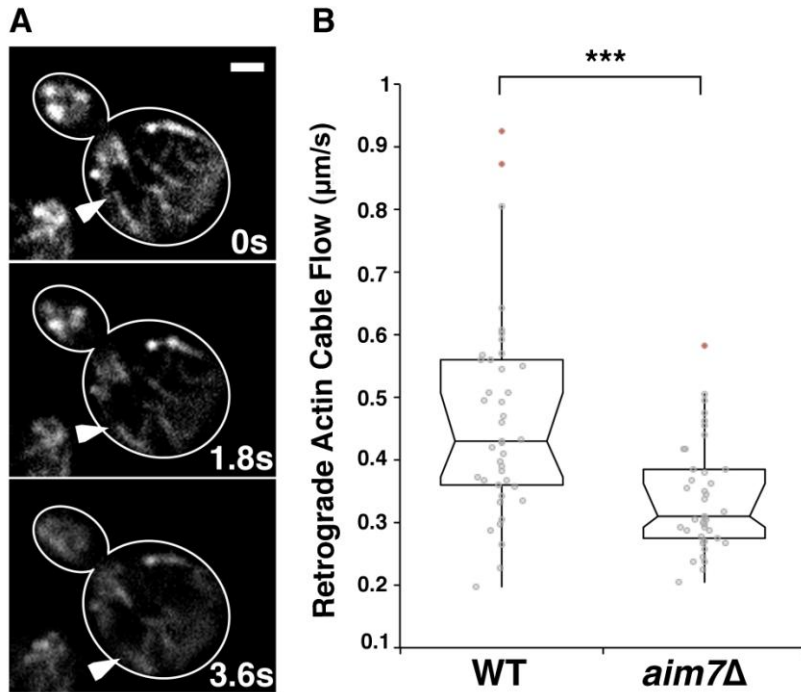


**Fig. 6** Deletion of *AIM7* results in decreased retrograde actin cable flow. **(A)** Still frames of a time-lapse series showing Abp140p-GFP-labeled actin cables undergoing retrograde flow. Arrowheads indicate a fiduciary mark on a motile actin cable. **(B)** Wild-type (BY4741) and *aim7* $\Delta$  cells with GFP-tagged Abp140p were grown to mid-log phase in lactate media, mounted on a coverslip, and imaged immediately for a maximum of 5 minutes. Notched dot box plot of the velocity of retrograde actin cable flow in wild-type and *aim7* $\Delta$  yeast. The central band in the box represents the median, boxes indicate the middle quartiles; whiskers extend to the 5-95%, and red points indicate outliers (defined as quartile 1 – 1.5x interquartile range and quartile 3 + 1.5x interquartile range). n = 40, pooled data from 3 trials.

### **3.3 Growth in Non-fermentable Carbon Sources Results in Upregulation of Mitochondrial Proteins and Increases in Actin Cable Thickness**

During growth in high concentrations of glucose, glycolysis is the primary mechanism of energy production and mitochondrial enzymatic action is limited. Under de-repressing conditions, such as growth in absence of glucose, mitochondrial biogenesis and enzymatic activity of key mitochondrial proteins are upregulated [27]. To determine the changes in mitochondrial biogenesis under growth in de-repressing conditions, we studied levels of  $\alpha$ -ketoglutarate, a mitochondrial matrix protein involved in the tricarboxylic acid cycle, in yeast cells grown in synthetic complete (2% glucose, SC), synthetic complete (2% raffinose), and lactate media. Here, SC represents growth under glucose repression; raffinose, which is enzymatically cleaved into glucose, galactose, and fructose represents low levels of glucose repression; and lactate represents complete de-repression. Consistent with previous work, we find that levels of  $\alpha$ -ketoglutarate increase in non-fermentable carbon sources, specifically 4-fold in raffinose and 5.5-fold in lactate (Fig. 7).

Since the actin cytoskeleton plays a pivotal role in mitochondrial movement, we speculate that changes in mitochondrial mass result in corresponding changes in the actin cytoskeleton. To study this, we measured actin cable abundance, actin polarity, and actin cable thickness in yeast grown in SC, raffinose, and lactate media. Indeed we see an increase in actin cable thickness in cells grown in raffinose and lactate media. Consistent with changes in levels of  $\alpha$ -ketoglutarate, actin cable thickness increases from 0.246 $\mu\text{m}$  in SC to 0.273 $\mu\text{m}$  in raffinose and 0.288 $\mu\text{m}$  in lactate (Fig. 8B). However, we detect no changes in actin cable abundance or defects in actin polarity in cells grown in either raffinose or lactate (Fig. 8C-D). This suggests that an increase in actin cable thickness is sufficient to meet the demands of increased mitochondrial mass.

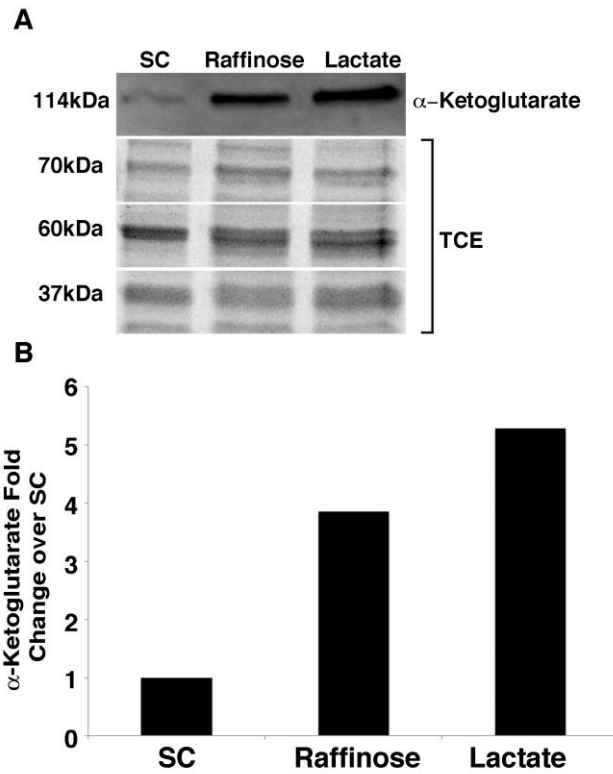


**Fig. 7** Wild-type (BY4741) cells grown to mid-log phase in SC, raffinose and lactate. Proteins were separated on SDS-PAGE and immunoblotted with an antibody raised against  $\alpha$ -ketoglutarate. Visualization of proteins using TCE in stain-free gel was used as a load control. **(A)** Representative blots from 3 independent experiments. **(B)** Quantitation of the amount of  $\alpha$ -ketoglutarate in each media compared to 3 protein bands labeled with TCE. Values are averages of the 3 quantifications.

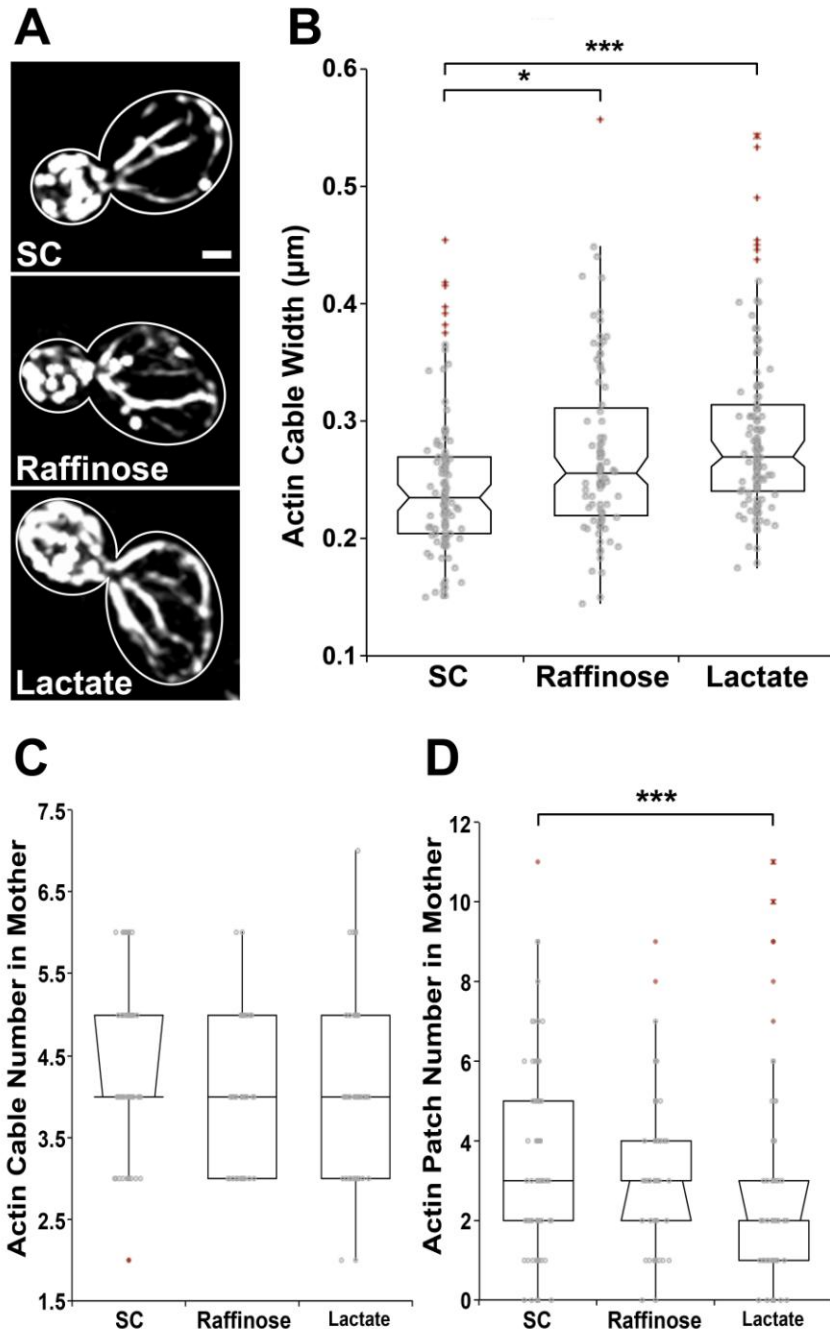


**Fig. 8** Growth in non-fermentable carbon source results in increased actin cable thickness, but does not alter actin cable abundance or actin polarity. Wild-type cells were grown to mid-log phase in glucose, raffinose, or lactate, fixed, and stained with rhodamine phalloidin. **(A)** Representative images of rhodamine-phalloidin stained actin of wild-type (BY4741) yeast in glucose, raffinose, and lactate media. **(B)** Thickness of actin cables was measured by drawing a line profile in ImageJ software. Line profiles are made through the ROI tool and drawn roughly perpendicular to the mother-bud axis near the middle of the mother cell, avoiding actin patches. We measured the width of the line profiles at half-max peak height, and acquire measurements of actin cable thickness in  $\mu\text{m}$ s. **(C)** Polarized actin cables were counted in mother cells as per Fig. 5. **(D)** The

number of actin patches in the mother is used as a measure of total cellular polarization with higher numbers in the mother indicating depolarization of actin. **(B-D)** Notched dot box plots where central bands in the box represent the median, boxes indicate the middle quartiles, and whiskers extend to the 5<sup>th</sup> and 95<sup>th</sup> percentile. Red points indicate outliers (defined as quartile 1 – 1.5x interquartile range and quartile 3 + 1.5x interquartile range). n = 85-124, representative data of 3 trials.

## 4 Conclusions and Further Directions

We find that Arp2/3 complex and Aim7p are important regulators of the dynamics of actin cytoskeleton-mitochondria interactions.

Deletion of the *ARC15* gene results in decreased actin cable abundance and loss of actin patches. This data provides evidence that the Arp2/3 complex is crucial for actin patch formation and maintenance of long, polarized cables. Deletion of *AIM7* results in decreased mitochondrial motility, decreased actin cable abundance, and loss of actin polarity. Furthermore, *aim7Δ* cells also have decreased retrograde actin cable flow. This observation also explains as to why *aim7Δ* cells exhibit decreased retrograde mitochondrial motility: decreased retrograde cable flow results in decreased retrograde mitochondrial motility.

To determine if changes in actin cable dynamics in *arc15Δ* cells correspond with alterations in mitochondrial motility, measurements of retrograde actin cable flow and both anterograde and retrograde mitochondrial velocity in the *arc15* deletion strain could be carried out. It would be interesting to investigate what the spatial and temporal requirements for Aim7p in mitochondria-actin interactions are. Do they colocalize with actin cables and mitochondria?

Due to release from glucose repression, growth on semi or non-fermentable carbon sources results in upregulation of mitochondrial proteins such as  $\alpha$ -Ketoglutarate. There is also an increase in actin cable thickness in non-fermentable carbon sources, suggesting that changes in actin cable thickness are essential to meet the demands of increased mitochondrial mass. However, actin cable number and actin polarity are not altered in non-fermentable carbon sources.

It would be interesting to see whether retrograde actin cable flow changes in varying media types. It would also be essential to look at mitochondrial quality, quantity and motility changes in different media types.

All in all, my observations suggest a mutual interdependence between the actin cytoskeleton and mitochondria: actin cytoskeleton affects mitochondrial distribution, and at the same time the level of mitochondria can also affect the actin cytoskeleton.



## **5 Acknowledgements**

I thank my principal investigator, Liza Pon, for all valuable inputs and comments throughout this project and for letting me be part of her lab. I also would like to thank my advisor Istvan Boldogh for all his guidance and for all his help with the report.

I also thank Ryo Higuchi for all his experimental support and for always having time for my questions. Thanks also to other members of the Pon laboratory for being so great and supportive.

I also wish to thank Leif Bülow for making my exchange work possible.

## 6 References

1. Boldogh, I.R., Yang, H-C. and Pon, L.A. (2001) Mitochondrial Inheritance in Budding Yeast. *Traffic*, 2(6), pp. 368-374
2. Boldogh, I.R., *et al.* (2004) A Type V Myosin (Myo2p) and a Rab-like G-Protein (Ypt11p) Are Required for Retention of Newly Inherited Mitochondria in Yeast Cells during Cell Division. *Molecular Biology of the Cell*, 15(9), pp. 3994-4002
3. Boldogh, I.R. and Pon, L.A. (2007) Purification and subfractionation of mitochondrial from the yeast *Saccharomyces cerevisiae*. *Methods in Cell Biology*, 80, pp. 45-64
4. Sherman, F. (2002) Getting started with Yeast. *Methods in Enzymology*, 32, pp. 3-41
5. Peraza-Reyes, L., Crider, D.G. and Pon, L.A. (2010) Mitochondrial manoeuvres: Latest insights and hypotheses on mitochondrial partitioning during mitosis in *Saccharomyces cerevisiae*. *Bioessays*, 32(12), pp. 1040-1049
6. Yamamoto, A. and Hiraoka, Y. (2003) Cytoplasmic dynein in fungi: insights from nuclear migration. *The Journal of Cell Science*, 116(22), pp. 4501-4512
7. Moseley, J.B. and Goode, B.L. (2006) The yeast actin cytoskeleton: from cellular function to biochemical mechanism. *Microbiology and Molecular Biology Reviews*, 70(3), pp. 605-645
8. Yang, H.C. and Pon, L.A. (2002) Actin cable dynamics in budding yeast. *Proceedings of the National Academy of Sciences of the United States of America*, 99(2), pp. 751-756
9. Boldogh, I.R. and Pon, L.A. (2006) Interactions of mitochondria with the actin cytoskeleton. *Biochimica et Biophysica Acta*, 1763(5-6), pp. 450-462
10. Fehrenbacher, K.L., *et al.* (2004) Live cell imaging of mitochondrial movement along actin cables in budding yeast. *Current Biology*, 14(22), pp 1996-2004
11. Hammer, J.A. 3rd and Sellers, J.R. (2012) Walking to work: roles for class V myosins as cargo transporters. *Nature reviews. Molecular Cell Biology*, 13(1), pp. 13-26

12. Boldogh, I.R., *et al.* (2001) Arp2/3 complex and actin dynamics are required for actin-based mitochondrial motility in yeast. *Proceedings of the National Academy of Sciences of the United States of America*, 98(6), pp. 3162-3167
13. Simon, V.R., *et al.* (1995) Actin-dependent mitochondrial motility in mitotic yeast and cell-free systems: identification of a motor activity on the mitochondrial surface. *The Journal of Cell Biology*, 130(2), pp. 345-354
14. Boldogh, I.R., *et al.* (2003) A protein complex containing Mdm10p, Mdm12p, and Mmm1p links mitochondrial membranes and DNA to the cytoskeleton-based segregation machinery. *Molecular Biology of the Cell*, 14(11), pp. 4618-4627
15. Kornmann, B., *et al.* (2009) An ER-mitochondria tethering complex revealed by a synthetic biology screen. *Science*, 325(5939), pp. 477-481
16. Millard, T.H., *et al.* (2004) Signalling to actin assembly via the WASP (Wiskott-Aldrich syndrome protein)-family proteins and the Arp2/3 complex. *The Biochemical Journal*, 380(1), pp. 1-17
17. Taunton, J., *et al.* (2000) Actin-dependent propulsion of endosomes and lysosomes by recruitment of N-WASP. *The Journal of Cell Biology*, 148(3), pp. 519-530
18. Gouin, E., *et al.* (2005) Actin-based motility of intracellular pathogens. *Current Opinion in Microbiology*, 8(1), pp. 35-45
19. Fehrenbacher, K.L., *et al.* (2005) A role for Jsn1p in recruiting the Arp2/3 complex to mitochondria in budding yeast. *Molecular Biology of the Cell*, 16(11), pp. 5094-5102
20. Hess, D.C., *et al.* (2009) Computationally driven, quantitative experiments discover genes required for mitochondrial biogenesis. *PLoS Genetics*, 5(3), e1000407
21. Pon, L.A., and Schatz, G. (1991) Biogenesis of yeast mitochondria, *The Molecular Biology of the Yeast Saccharomyces*, Broach, J.R., Pringle, J.R. and Jones, E.W., Cold Spring Harbor, New York
22. Ulery, T.L., Jang, S.H. and Jaehning, J.A. (1994) Glucose repression of yeast mitochondrial transcription: kinetics of derepression and role of nuclear genes. *Molecular and Cellular Biology*, 14(2), pp. 1160-1170

23. Lazzarino D.A., *et al.* (1994) Yeast mitochondria contain ATP-sensitive, reversible actin-binding activity. *Molecular Biology of the Cell*, 5(7), pp. 807-18
24. Ladner, C., *et al.* (2003) Visible fluorescent detection of proteins in polyacrylamide gels without staining. *Analytical Biochemistry*, 326(1), pp. 13-20
25. Fehrenbacher, K., *et al.* (2003) Actin comet tails, endosomes and endosymbionts. *The Journal of Experimental Biology*, 206(12), pp. 1977-1984
26. Gandhi, M., *et al.* (2010) GMF is a cofilin homolog that binds Arp2/3 complex to stimulate filament debranching and inhibit actin nucleation. *Current Biology*, 20(9), pp. 861-867
27. Falcone, C., Agostinelli, M. and Frontali, L. (1983) Mitochondrial translation products during release from glucose repression in *Saccharomyces cerevisiae*. *Journal of Bacteriology*, 153(3), pp. 1125-1132
28. de Maré, S. (2012) The role of Aim7p in mitochondrial inheritance in budding yeast. *Master Thesis, Lund University*, pp. 1-24